ISSN No.: 2455-6130
Special Issue: I, 2022, pp. 99-112

website: www.ijoetr.com

International Journal of Emerging Trends in Research

STUDY ON MECHANICAL AND MICROSTRUCTURAL PROPERTIES OF TI– ALLOYS PRODUCED BY DIRECT METAL DEPOSITION

Pratheesh Kumar S*, Rajesh R, Raja V, Manojh Kumar R

Deptt. of Prod. Engg. PSG College of Technology, Coimbatore

Abstract

The term "additive manufacturing" (AM) refers to a procedure in which parts are created by layering them together. Metal AM, also referred as Direct Metal Deposition (DMD), has progressed significantly in recent years to be a revolutionary technology that can change the way objects from a variety of sectors are created. On the other hand, comprehensive and in-depth analyses of the mechanical characteristics and microstructure of metals and alloys made using AM are uncommon. A thorough understanding of the microstructure and mechanical attributes of metal AM-produced parts is necessary to effectively exploit metal additive manufacturing's design potential. The mechanical characteristics and microstructure of metal deposited components were studied in this article. The relationship between mechanical qualities and microstructural characteristics such as strength and hardness and process parameters has been researched for a variety of materials. This research aids in determining the appropriate process parameters for the material selected, allowing for the achievement of the desired output characteristics for the specified applications.

Keywords: additive manufacturing; direct metal deposition; microstructure; strength;

1. Introduction

The term Additive Manufacturing (AM) refers to the process of producing products layer by layer. It permits the on-demand creation of three-dimensional objects. AM refers to a diverse range of manufacturing techniques with the capacity of processing a variety of materials such as ceramics, polymers, and metals [1]. AM has the potential to revolutionize the way goods are conceived and manufactured. Generally, product-specific tooling can be omitted with AM, and enable the creation of very complex geometries that condense numerous pieces, are more resourceful, and blend materials in formerly inconceivable manners [2]. Based on the American Society for Testing and Materials (ASTM), AM is a technique of combining materials to create items based on data from 3D models, often layer after layer, in contrast to subtractive fabrication techniques including conventional machining. It is progressively gaining traction in aerospace, racing, toys, and jewellery, as well as a variety of medical applications that require high levels of customization [3]. Stereolithography (SL) from 3D Systems pioneered additive manufacturing in 1987, a method that uses a laser to harden thin layers of UV light-sensitive fluid polymers [4].

Direct Metal Deposition (DMD) is an AM procedure that assists in the production of near-net-shape parts by melting metal powder, wires, or ribbon and consecutively layering them onto a workpiece. A focused laser heat source is utilized in this process for melting the metallic feedstock and molds it into the desired shape, as illustrated in Fig. 1. DMD enables the fabrication of a complete dense-metal component with the desired functional qualities in a fraction of the time,

with less raw material waste, and at a fraction of the cost of existing techniques. The powdered building material is delivered into the pool by an inert gas stream, which causes it to expand in size. Typically, the process is shielded from damaging oxidation by the inert gas stream or by confining it in a room saturated with an inert gas such as nitrogen or argon [5]. Part solidification and quick melting are combined with intense at the solid or liquid boundary, supercooling occurs throughout the DMD process. [6].

The DMD method has several advantages, which are listed below. DMD is primarily used for structure generation from scratch. Additionally, it is used to fix an existing structure or component. Large components can be easily made. It produces at a faster rate than other additive manufacturing technologies like as SLM and EBM, provides fabrication freedom for components. When used along with a robotic arm, this approach enables the fabrication of complicated part features with near net or net shaped capabilities. Due to the layered manufacturing method and the capability of handling various powders, this procedure enables the creation of multifunctional homogenous or heterogeneous structures, applied to a wide array of materials with a diversity of morphologies [7, 8].

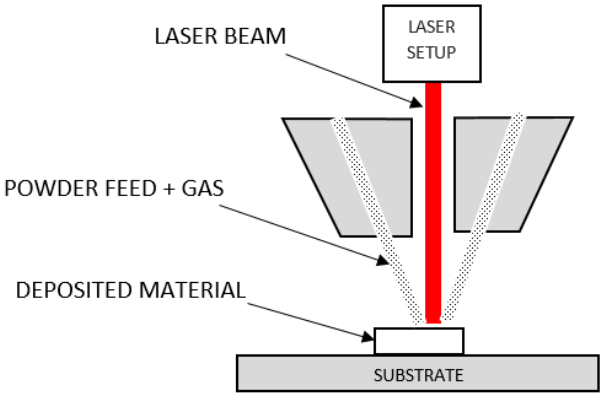

Fig. 1 Schematic representation of DMD

The following are the downsides of the DMD process. Direct energy deposition (DED) devices are prohibitively expensive in comparison to other methods of metal AM. Due to the absence of support structures, fabricating features such as overhangs will be significantly more challenging. It cannot be used in large-scale manufacturing. This procedure is unrepeatable, problematic to attain adaptive control, requires time-consuming and costly post-process inspection, and generates accumulative mistake. These difficulties continue to obstruct DED's widespread adoption and full realization of its promise [9].

2. Types of DMD

DMD is primarily classified according to its energy source and feed mechanism. Commercially accessible DMD systems utilize a range of heat sources, considering laser, electron beam, and plasma arc, for melting the feedstock (powder or wire) [12].

Laser assisted DMD is a layer-by-layer manufacturing process for creating components from a CAD (computer-aided design) model. Laser assisted DMD is among the very first DED technologies to be commercialized. It was made by Sandia National Laboratories in the United States of America (USA) and commercialization was done by Optomec in the USA. Optomec introduced the "Laser engineered net shaping (LENS) 750" machine in 1997. In a confined inert gas container, LENS machines process materials. This system is hundreds of times more efficient

than the inert gas devices employed in powder beds. The five-axis "laser wrist" devices allow for deposition from any angle, as well as monitoring techniques for melt pool region and build height can be utilized flexibly in order to preserve deposit features that are constant [10].

NASA Langley, USA, designed Electron Beam Freeform (EBF) fabrication as a method for fabricating and/or repairing structures in the aircraft industry on Earth as well as in upcoming space-based solutions [12]. Employing a wire feeder and an electron beam as a heating element, EBF can deposition quickly when there are strong currents or deposition very precisely at low pace. Electron beams show significantly higher efficiency surpasses most lasers at conversion of electrical energy to a beam, thereby conserving sparse electrical assets; These machines excel at rapidly forming big, bulky deposits, allowing for the production of huge deposits such as rib-on-plate structures and others (usually for aerospace applications), hence reducing the lengthy lead times associated with their forged counterparts [11].

Plasma is one of matter's four fundamental states. It is composition of a gas of ions. Because of the availability of free charged particles, plasma is electrically conductive; individual particle behaviors and macroscopic plasma movement are governed by collective electromagnetic fields and are particularly sensitive to artificially created fields. These technologies are practical and beneficial as less expensive choices to laser and electron beam modes of fabrication, but difficulties in the control aspects of the process have prevented extensive commercialization [11].

Metal powder and metal wire are often used additive materials in DMD. According to the method through which the additive material is provided, DMD technologies can be classified as powder- or wire-feed. As illustrated in Fig.1, the powder feed system delivers the powder to a laser-generated melt pool on a metallic substrate. Several drawbacks of this method, including a low deposition rate, difficulty to enhance the efficiency of the catchment, and the frequently produced poor-quality surface finish [13].

In wire-feed technology, the supply material is a metal wire rather than metal powder as shown in Fig. 2. Wire-feed systems maximize material utilization so that almost all of the wire filament material is deposited into the part. It has a higher deposition rate than the powder-feed technique. Wire feed AM is a versatile method able to produce diverse variety of metals and alloys. There is largely material- and process-dependent concerns that are influenced among various wire qualities (e.g., diameter and chemical composition) as well as operating variables (e.g., weld speed, wire feed rate, wire feeding angle and direction, and laser power). Several problems have been discovered when wire is employed as the supplementary material, such as residual stress and deformation induced by excessive heat input, relatively low part precision, and a lack of surface polish on the manufactured components [14, 15].

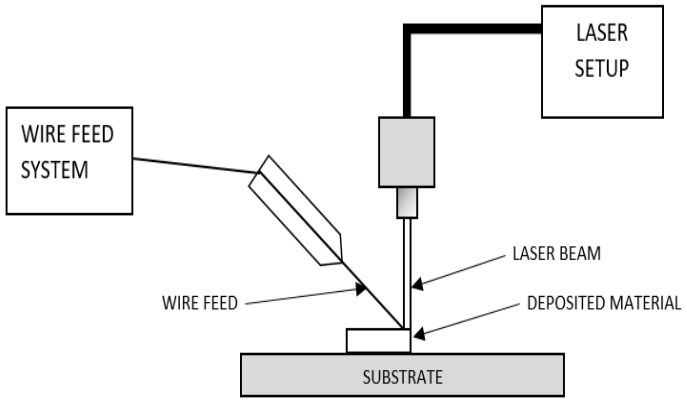

Fig. 2 Schematic representation of direct wire fed deposition system

3. Influencing process parameters in DMD

The scanning velocity, rate of powder flow, laser power, and flow rate of gas are the primary DMD process factors that affect component characteristics. Due to the highly interacting nature of these process factors, the LMD process is an extremely sensitive device. Understanding the impact of a single operating parameter on output qualities will aid in efficiently regulating these features in such a sensitive system.

The power of the laser used has a major consequence on the properties of the deposited metals. The laser power provided may be either continuous or pulsed [16]. The floating powder particles' scattering, absorption, and melting capabilities absorbed and dispersed all of the laser energy, preventing the substrate from remelting. On the other hand, the melt pool penetrated further into the substrate as the laser power was raised. In this case, the laser energy delivered at medium-high power levels adequately covered powder dissipations and allowed for substrate remelting, guaranteeing strong metal bonding between the as-deposited and the substrate material [16, 17].

The standoff distance, is a term used to describe the separation between the deposition point and nozzle. It is a critical process parameter. The experimental results indicate that when the standoff distance between the outlet of nozzle and the powder focal point is less compared to powder focal length, the variations of thin-wall parts' top surfaces can be automatically adjusted on subsequent layers, but while the standoff distance is equal to or greater than the focal length of powder, the outcomes are poor [18]. If the standoff distance equals the powder focus length, there is a maximal building height [19].

When the flow rate of powder is low, the amount of powder transported to the laser beam generated melt pool on the substrate is small, allowing for efficient melting. The melt pool formed is big due to the high value of laser power and the small value of the powder delivered, which led to greater melting of the substrate's surface. At increased powder flow rates, the huge amount of available powder for melting precludes significant melting of the substrate materials, as the delivered powder consumes a significant portion of the available laser power. The micro hardness of the powder improved as the flow rate of powder raised. The low value of microhardness observed at low powder flow rates was caused by the soft basket woven alpha grain structure generated by the large melt pool at low powder flow rates [20].

The scanning speed of a laser is defined as the velocity with which it moves across a substrate. Microhardness increases in lockstep with scanning velocity. Additionally, as the velocity of scanning was incremented, the wear resistance of the samples was incremented [21]. The thickness initially increased when the velocity of scanning increased, but then began to decrease [22]. If the powder flow rate was fixed, the composite layer's overall size was reduced. The thickness of dilution was discovered to reduce with increase in scanning velocity [23].

DMD is an intriguing new process with significant application potential in a variety of fields, as with any other additive manufacturing technique, the characteristics of a DMD-produced part are heavily dependent on the input process variables that affect the grain structure of the part and thus its mechanical properties such as strength, toughness, and so on. Thus, it is critical to understand how output characteristics change as a function of parameters used in the process for various materials. The following literature information, summarized in the tables below, aids in a deeper comprehension of how output process factors vary in response to changes in the process's input variables.

Lu et al. [24] examined the mechanical characteristics and microstructure of Ti6Al4V in both Z and X direction. The x-direction microstructure consists of phases with prior grains with delicate grain boundaries and short, thin columns while the z-direction microstructure contains small colonies with short plates and lengthy columnar preceding grains parallel to tensile plane. In the x-direction, the yield strength and UTS are 922.6 MPa and 992.8 MPa, respectively, which is

superior. Lu et al. [27] examined the mechanical characteristics and microstructure of the NiTi alloy. Under constant process conditions, a large columnar grain structure with average NiTi alloy lengths is observed. The mechanical attributes and microstructure of Ti-15Mo have been discussed by H Tan et al. [28]. The microstructure of the DMD Ti-15Mo specimen is characterized by grains that are finely equiaxed or close to being equiaxed. The material has outstanding compressive qualities and a 1764 MPa of tensile strength, according to compression test findings. By varying the scanning speed and wire feed rate while maintaining all other parameters constant.

Baufeld et al. [26] investigated Ti6Al4V microstructure and mechanical characteristics were examined. A fine Widmanstatten structure exhibited in top region, while the coarse Widmanstatten structure exhibited in bottom region. The UTS ranges from 929 to 1014 MPa, and the obtained hardness values range from 3.2 to 3.7 GPa. This demonstrates that the mechanical properties of Ti6Al4V vary according to the rate of wire feeding. P. Akerfeldt et al. [29] discussed the mechanical properties and microstructure of the Ti-6Al-4V alloy. Two distinct samples, one with continuous deposition and the other with layers separated by a pause. Perpendicular specimens were positioned across the preceding beta grains, whereas parallel specimens were placed perpendicular to the prior beta grains. The sample with a 2 to 3 minute rest period between layers was found to have superior properties to the continuous sample.

S Liu and Y C Shin [30] investigated the microstructure and mechanical properties of a composite composed of Ti6Al4V and TiC. The percentage of TiC varied between 0% and 15% in the LDD Ti64-TiC MMCs' microstructures. The addition of TiC considerably affected the microstructure of Ti64 matrix when compared to LDD Ti64. A lamellar structure that is very short and frail was created instead of the acicular martensite. It was discovered that the sample containing 15% TiC possessed superior mechanical properties. H. S. Ren et al. [31] discussed the mechanical properties and microstructure of Ti–6.5Al–3.5Mo–1.5Zr–0.3Si Graded Structural Material. Microhardness and microstructure values in the gradient zone gradually increase as the number of layers increases. Mechanical behaviour of the graded structural material is also analysed during a room temperature tensile test, with yield and ultimate strengths of 880 ± 4 MPa and 933 ± 3 MPa, respectively.

Y. Liu and Y. Zhang [32] examined the evolution of the microstructure and mechanical properties of bimetallic samples TA15-Ti2AlNb. The diffusion zone's microstructure has a distinct interface. Diffusion zone I contains the acicular phase in coarse form, while diffusion region II contains the needle 2 phase. The phase change from the TA15 alloy to Ti2AlNb-based alloy is as follows: α (lath) +α (coarse acicular) +β→β+α2→α2+O+B2. The first region's hardness value is less than the second region. F Zhang et al. [33] investigated the microstructure and mechanical behaviour of samples of Ti-2Al-yMo (y = 2, 5, 7, 9, 12) alloy. Large columnar grains develop small equiaxed granules epitaxially towards the top of the deposited layers. Suo et al. [34] discussed the microstructure and mechanical characteristics of Ti6Al4V, which was synthesized with the help of an electron beam. Large columnar grains describe the microstructure over multiple deposition levels. This demonstrates that the mechanical properties along the X-axis are superior to those along the Z-axis. B Lu et al. examined the microstructure and mechanical behaviour of TiNi alloy formed via Plasma Arc Deposition. At top, middle and bottom of microstructure of TiNi alloys, TiNi dendrite crystals, TiNi equiaxed crystals, and TiNi cellular crystals were observed. The as-deposited samples had a good hardness (390 HV) and a high UTS value (1604 MPa). J. J. Lin et al. [35] examined the mechanical behavior and microstructure of Ti-6Al-4V generated through an AM method utilising pulsed plasma arcs (PPAM). Variable previous columnar big grains develop virtually perpendicularly over many layers were deposited from substrate to top layer. By lowering the microstructure of the thin wall was optimised in PPAM process by adjusting the pulsed current is used to heat each bead.

Table 1: Powder Feed-based Materials

Material	Laser Power (W)	Scan Speed (m/min)	Powder Flow Rate (g/min)	Standoff Distance (mm)	Microstructure Observed	YS (MPa)	UTS (MPa)	Hardness	Ref.
Ti6Al4V	170	1.25	-	-	Delicate grain boundaries and small, narrow columnar prior grains that developed along the x axis. Small colonies with short plates and long columnar preceding grains direction.	922.6 (X), 868 (Z)	992.8 (X), 956.8 (Z)	-	[25]
NiTi alloy	1300	0.72	8	-	The deposited NiTi alloy has typical lengths of huge columnar grains. Along the path of construction, those columnar grains develop epitaxially.	482.4 ± 110	772 ± 90	323 ± 30 HV	[27]
Ti-15Mo	1500	0.48	20	-	Smaller size equiaxed grains with no obvious substructure were uniformly dispersed at top of each Ti-15Mo deposited layer, whereas small size near-equiaxed grains were detected with cellular substructure distributed at bottom.	1172.5 - 1176.1	1718.1 - 1799.1	-	[28]

Table 2: Wire Feed-based Materials

Material	Laser Power (W)	Scan Speed (m/min)	Wire Feed Rate (m/min)	Standoff Distance (mm)	Microstructure Observed	YS (MPa)	UTS (MPa)	Hardness	Ref.
Ti6Al4V	-	0.1 - 0.4	0.6 - 7.7	-	The top region has a fine Widmanstätten structure (phase colony or basket structure in phase matrix) and the bottom part has a coarseWidmanstätten structure.	-	929 - 1014	3.2 - 3.7 GPa	[26]

Ti6Al4V	2000 - 3000 V	-	0.6	-	During manufacturing, enormous columnar prior beta grains occur in the microstructure of the deposited Ti-6Al-4V. The parallel samples were across the preceding beta grains, while the perpendicular specimens were beside them.	790 - 925	880 - 980	345 ± 16 HV	[29]
Ti6Al4V (0 - 15%) + TiC	200 - 375	0.9	1.2 - 2	-	In titanium alloys, the high cooling rate during LDD manufacturing always leads to the formation of acicular martensite,the LDD Ti64-TiC MMCs' microstructures. In comparison to LDDTi64, the TiC significantly altered the microstructure of the Ti64 matrix. A lamellar + structure that is narrow and short was created instead of the acicular martensite.	997 - 1310	1381 - 1636	39 - 55	[30]

Table 3: Laser Beam-based Materials

Material	Laser Power (W)	Scan Speed (m/min)	Powder Flow Rate (g/min)	Microstructure Observed	YS (MPa)	UTS (MPa)	Hardness	Ref.
TA15-Ti2AlNb bimetallic structure	1000	0.3 (TA15), 0.24 (Ti2AlNb)	2.9 - 3.7	In diffusion region I, the coarse acicular phase shows, while in diffusion region II, the needle 2 phase appears. From the TA15 alloy side to the Ti2AlNb-based alloy side, the phase change isα (lath) +β→α (coarse acicular) +β→β+α2→α2+O+B2.	-	1025	398- 447 HV	[32]
GSM of Ti-6.5Al-3.5Mo-1.5Zr-0.3Si	8000	-	-	Ti-6.5Al-3.5Mo-1.5Zr-0.3Si contains more β-stable elements.Becauseof the enlarged laths interfaces, the volume fraction of phase increases. On further layers, α phase decreases further.	880 ± 4	933 ± 5	350 - 390 HV	[31]

Ti-2Al-yMo (y = 2, 5, 7, 9, 12)	2800 - 3000	0.4	4.5	Big columnar grains develop epitaxially with small equiaxed grains, with the thickness of the equiaxed grain layer being proportionate to the Mo concentration.	650 - 850	800 - 950	250 - 525 HV	[30]

Table 4: Electron Beam-based Materials

Material	Beam Current (mA)	Power (kV)	Scan Speed (m/min)	Powder Flow Rate (g/min)	Microstructure Observed	Standoff Distance (mm)	YS (MPa)	UTS (MPa)	Ref.
Ti6Al4V	35	60	0.35	0.9	Multiple deposition layers have large columnar grains, with bright and dark banded textures at the interlayer and interbead margins.	0.3	799 (X), 765 (Z)	899 (X), 855 (Z)	[34]

Table 5: Plasma Arc-based Materials

Material	Current (A)	Scan Speed (m/min)	Wire / Powder Feed Rate	Microstructure Observed	Hardness	YS (MPa)	UTS (MPa)	Pulse Frequency (Hz)	Duty Cycle (%)	Ref.
TiNi alloy	150	0.18	3.5 g/min	There were TiNi cellular crystals, dendritic crystals, and equiaxed crystals in the top, middle, and bottom of the microstructure of TiNi alloys, respectively.	390 HV	-	1604	-	-	[33]
Ti6Al4V	230 - 250 (peak)	0.25	3.5 m/min	Starting with the substrate and working up to the top layer, varying columnar β grains grow perpendicularly. After four layers, the columnar- β grain epitaxially grows in opposite orientations.	330 - 370 HV	909 ± 13.6	988 ± 19.2	70	30 - 50	[35]

According to the literature reviewed, output parameters such as the microstructure and mechanical properties of the parts vary in response to changes in process parameters. When materials were subjected to post-heat treatment, their mechanical properties improved. Additionally, it should be noted that components with a microstructure parallel to the lay direction exhibited superior mechanical properties. The research gap addressed is the lack of a thorough understanding of the microstructure and mechanical properties of deposited materials, because yield strength (YS) and ultimate tensile strength (UTS) are two input factors have an effect on the design aspects of a wide variety of materials. Layer by layer, the microstructure is created in metal AM. Therefore, comprehending the evolution of microstructure and resulting mechanical properties will aid in achieving the component's desired properties during fabrication.

4. Microstructure and mechanical properties

The data displayed in Table 2 reveals the variation in material properties with respect to the wire feed system when process parameters are varied. When the input parameters are 100 A, 10.2 V, and 0.7 m/min for Ti6Al4V, the diameter of the prior beta grains is significantly larger for these parameters. The yield strength was 895.18 MPa and the UTS was 956.618 MPa. Similarly, changing the parameters to 134 A, 11.8 V, and 1.8 m/min results in smaller, finer prior beta grains. The yield strength was 899.2 MPa and the UTS was 970 13 MPa, as shown in Fig.3. Similarly, when the scanning speed of the same material was varied from 0.1 to 0.4 m/min, a fine Widmanstätten structure was discovered in highest region and a coarse Widmanstätten structure in lowest section. When continuous deposition is used, the yield strength and UTS of the same material are 800 MPa and 880 MPa, respectively. When deposition is paused for two to three minutes between layers, yield strength and UTS are 925 and 980 MPa, respectively. The microstructure and mechanical properties of Ti6Al4V-TiC alloys change as the TiC content increases. The existence of TiC significantly alters the microstructure of Ti64 matrix. Rather than the acicular martensite, a lamellar + structure that is narrow and short was created. However, The Ti64 matrix returns to a fine structure as further TiC is introduced with a b1 m thick-lath and a shorter length.

When the percentage of TiC is varied between 0% and 15%, the yield strength ranges from 997 to 1310 MPa and the UTS ranges from 1381 to 1636 MPa. Mechanical properties increased as TiC percent increased. The data displayed in Table 3 reveals that the properties of materials vary according to the laser beam powered system's process parameters. When the Mo is varied between 2, 5, 7, 9, and 12, the Ti-2Al-xMo structure is obtained. The size of the primary and secondary laths decreases as the Mo content multiplies, whereas the volume fraction of secondary laths increases. The acicular martensite phase formed within the preceding grains is the martensite. The hardness ranges from 275 to 525 HV and increases as the Mo content grows. Tensile properties continue to increase until they reach a maximum value at 9 Mo. Tensile properties then decrease at 12Mo, as illustrated in Fig. 5. The following section discusses the variation in material properties in an electron beam deposition system displayed in Table 4 as a function of various process parameters. EBM of Ti6Al4V results in a prior β grain structure that is very columnar transforms into a diffusional α + β bulk microstructure. The following section discusses the variation in material properties in the plasma arc deposition system displayed in Table 5 as a function of various process parameters. When the current is varied between 230 and 250 A (peak), the yield strength and UTS of Ti-6Al-4V vary between 909 ± 13.6 MPa and 988 ± 19.2 MPa, respectively.

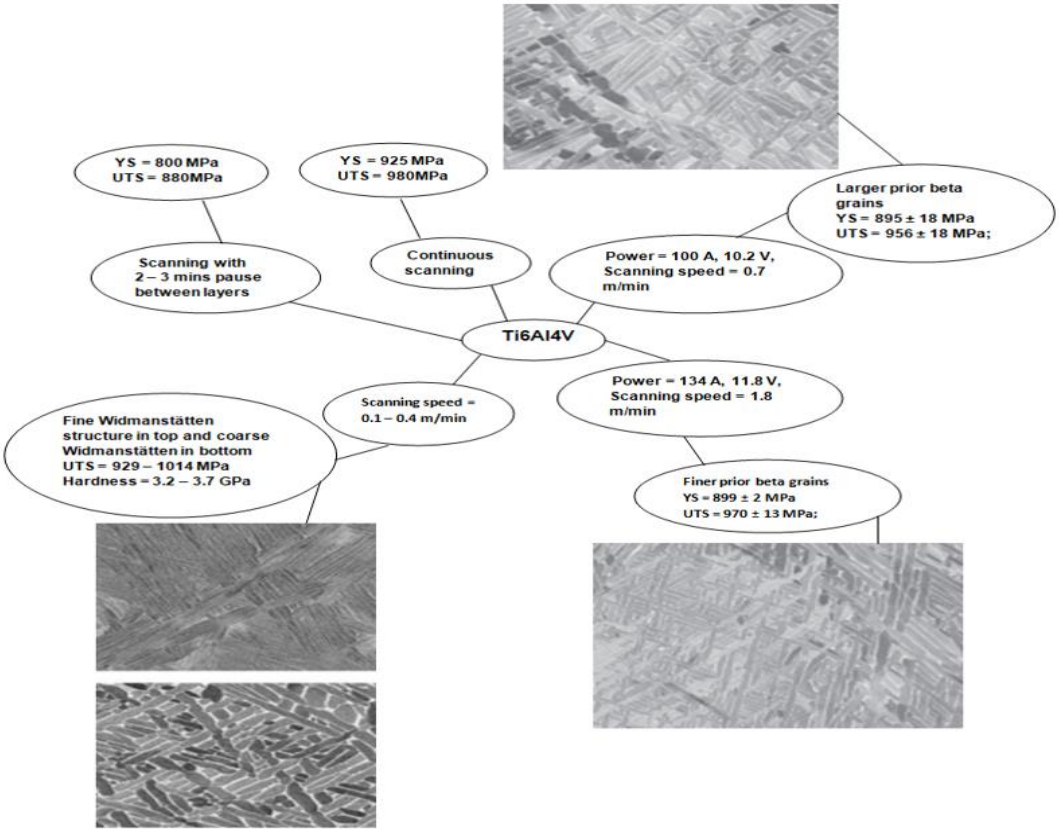

Fig. 3 Impact of process parameters on Ti6Al4V

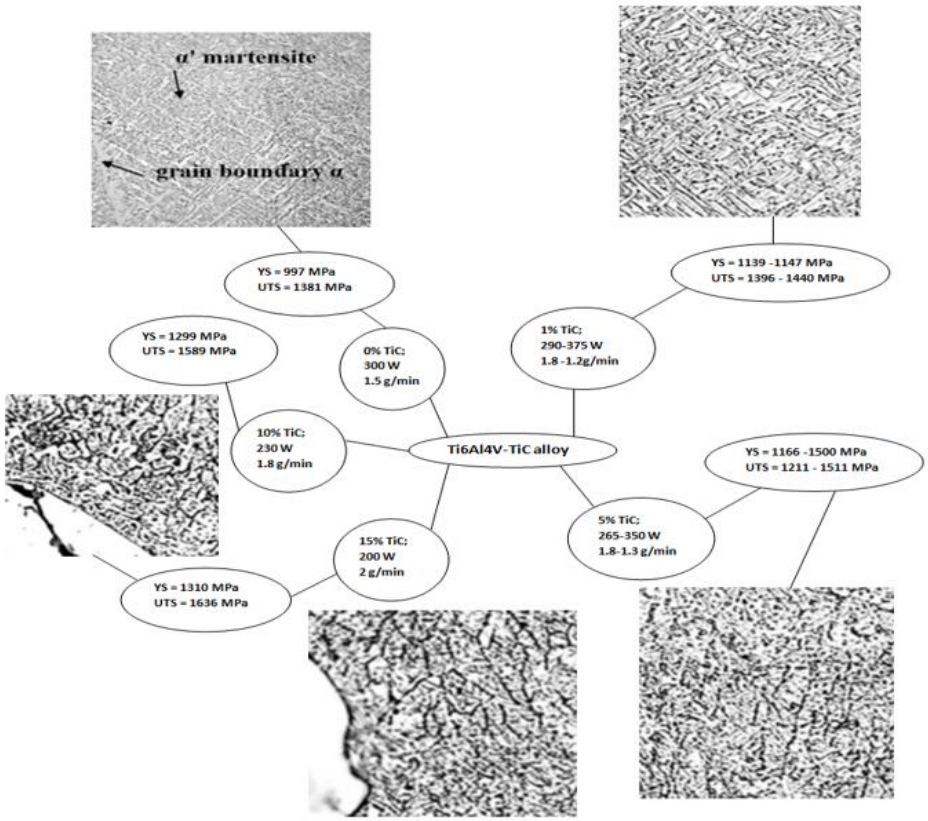

Fig. 4 Impact of process parameters on Ti6Al4V- TiC alloy

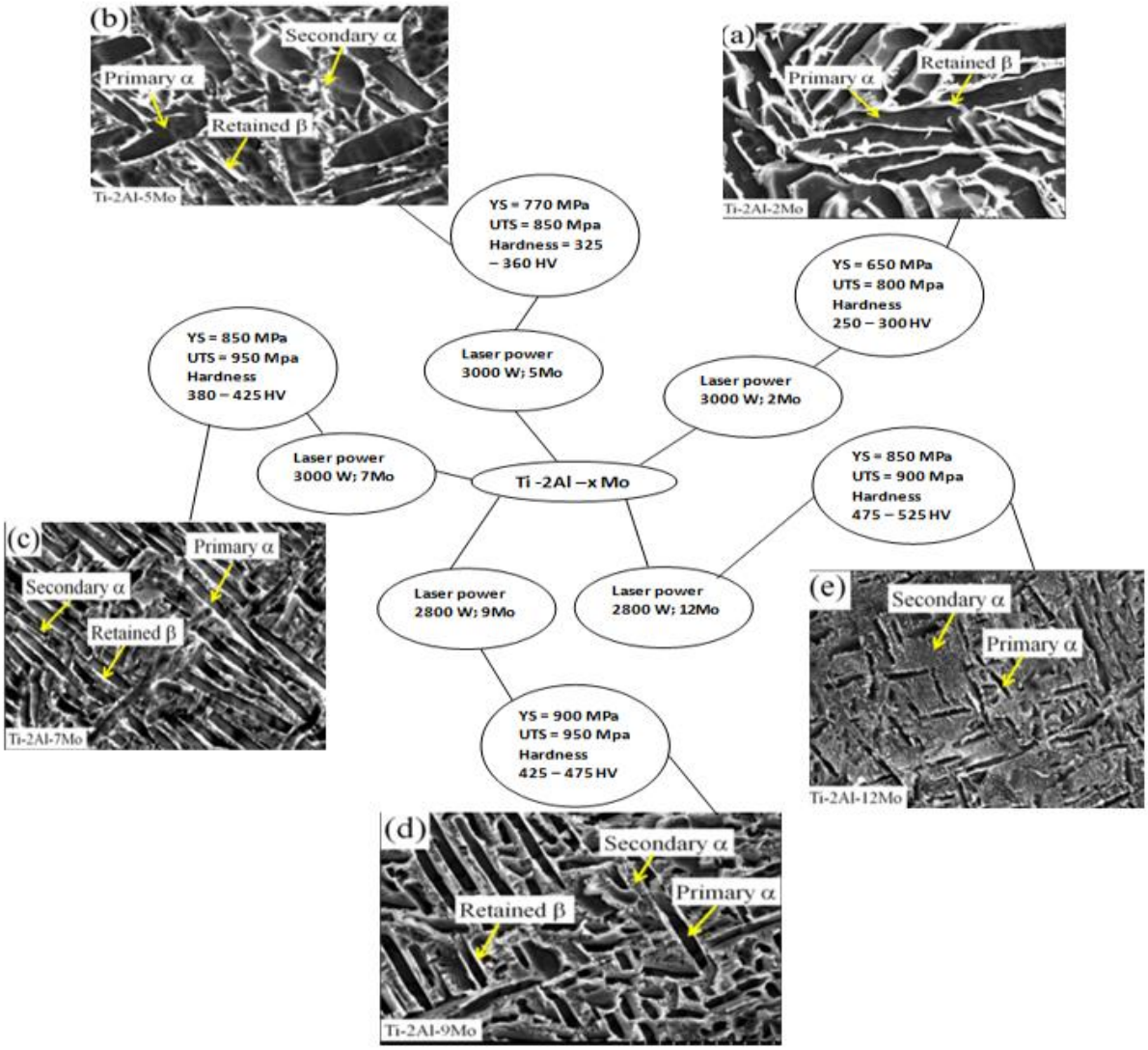

Fig. 5 Impact of process parameters on Ti-2Al-xMo

5. Conclusion

The microstructure of a component has a significant impact on the deposited part's characteristics, particularly its mechanical properties. This work examines the microstructure and resulting mechanical attributes of the deposited parts. This investigation was conducted on a variety of materials for ascertaining the resulting microstructure and mechanical properties for the specified process parameters. This study aids in forecasting the optimal process parameters for fabricating deposited materials used in a variety of applications. This study yields the following significant findings.

- The region near the bottom, close to the substrate, has improved mechanical properties during the direct metal deposition process.
- Laser power, particle deposition rate, and scanning speed all have a substantial impact on the microstructure of the deposited part.
- When a pause is allowed for deposition between layers, the deposited material's mechanical properties are enhanced.

- When wire feed deposition is used, the double wire-feed method results in components with improved mechanical properties.
- The process parameters must be chosen in accordance with the intended use of the deposited material. Thus, high values of strength and hardness can be obtained using a high laser power and a high deposition rate.

References

[1] S. S. Panse and S. V. Ekkad, "Forced convection cooling of additively manufactured single and double layer enhanced microchannels," Int. J. Heat Mass Transf., vol. 168, no. 120881, p. 120881, Apr. 2021.

[2] T. Peng, Y. Zhu, M. Leu, and D. Bourell, "Additive manufacturing-enabled design, manufacturing, and lifecycle performance," Additive Manufacturing, vol. 36. p. 101646, 2020.

[3] M. Despeisse and S. Ford, "The role of additive manufacturing in improving resource efficiency and sustainability," in Advances in Production Management Systems: Innovative Production Management Towards Sustainable Growth, Cham: Springer International Publishing, 2015, pp. 129–136.

[4] S. Pratheesh Kumar, S. Elangovan, R. Mohanraj, and J. R. Ramakrishna, "Review on the evolution and technology of State-of-the-Art metal additive manufacturing processes," Mater. Today, Mar. 2021.

[5] T. T. Wohlers and Wohlers Associates, Wohlers Report 2014: 3D Printing and Additive Manufacturing State of the Industry Annual Worldwide Progress Report. 2014.

[6] M. Brandt, Laser Additive Manufacturing: Materials, Design, Technologies, and Applications. Woodhead Publishing, 2016.

[7] J. Lu, L. Chang, J. Wang, L. Sang, S. Wu, and Y. Zhang, "In-situ investigation of the anisotropic mechanical properties of laser direct metal deposition Ti6Al4V alloy," Mater. Sci. Eng. A Struct. Mater., vol. 712, pp. 199–205, Jan. 2018.

[8] C. Wen, Metallic Biomaterials Processing and Medical Device Manufacturing. Woodhead Publishing, 2020.

[9] Z.-J. Tang et al., "A review on in situ monitoring technology for directed energy deposition of metals," The International Journal of Advanced Manufacturing Technology, vol. 108, no. 11–12. pp. 3437–3463, 2020.

[10] W.-W. Liu, Z.-J. Tang, X.-Y. Liu, H.-J. Wang, and H.-C.Zhang, "A Review on In-situ Monitoring and Adaptive Control Technology for Laser Cladding Remanufacturing," Procedia CIRP, vol. 61. pp. 235–240, 2017.

[11] B. Dutta, "Directed Energy Deposition (DED) Technology," Reference Module in Materials Science and Materials Engineering. 2020.

[12] J. Pinkerton, "Advances in the modeling of laser direct metal deposition," Journal of Laser Applications, vol. 27, no. S1. p. S15001, 2015.

[13] Gibson, D. Rosen, and B. Stucker, "Development of Additive Manufacturing Technology," Additive Manufacturing Technologies. pp. 19–42, 2015.

[14] W. U. H. Syed, A. J. Pinkerton, and L. Li, "Simultaneous wire- and powder-feed direct metal deposition: An investigation of the process characteristics andcomparison with single-feed methods," Journal of Laser Applications, vol. 18, no. 1. pp. 65–72, 2006.

[15] D. Ding, Z. Pan, D. Cuiuri, and H. Li, "Wire-feed additive manufacturing of metal components: technologies, developments and future interests," The International Journal of Advanced Manufacturing Technology, vol. 81, no. 1–4. pp. 465–481, 2015.

[16] W. Huang, S. Chen, J. Xiao, X. Jiang, and Y. Jia, "Laser wire-feed metal additive

manufacturing of the Al alloy," Optics & Laser Technology, vol. 134. p. 106627, 2021.
[17] S. Pratheesh Kumar, S. Elangovan, R. Mohanraj, and V. Sathya Narayanan, "Significance of continuous wave and pulsed wave laser in direct metal deposition," Mater. Today, Mar. 2021,
[18] S. Pratheesh Kumar, S. Elangovan, R. Mohanraj, and J. R. Ramakrishna, "A review on properties of Inconel 625 and Inconel 718 fabricated using direct energy deposition," Mater. Today, Mar. 2021.
[19] J. Pinkerton and L. Li, "The significance of deposition point standoff variations in multiple-layer coaxial laser cladding (coaxial cladding standoff effects)," International Journal of Machine Tools and Manufacture, vol. 44, no. 6. pp. 573–584, 2004
[20] G. Zhu, D. Li, A. Zhang, G. Pi, and Y. Tang, "The influence of standoff variations on the forming accuracy in laser direct metal deposition," Rapid Prototyping Journal, vol. 17, no. 2. pp. 98–106, 2011.
[21] R. M. Mahamood, E. T. Akinlabi, M. Shukla, and S. Pityana, "Scanning velocity influence on microstructure, microhardness and wear resistance performance of laser deposited Ti6Al4V/TiC composite," Materials & Design, vol. 50. pp. 656–666, 2013.
[22] S. P. Kumar, S. Elangovan, R. Mohanraj, and B. Srihari, "Critical review of off-axial nozzle and coaxial nozzle for powder metal deposition," Mater. Today, Mar. 2021
[23] T. Amine, J. W. Newkirk, and F. Liou, "Investigation of effect of process parameters on multilayer builds by direct metal deposition," Applied Thermal Engineering, vol. 73, no. 1. pp. 500–511, 2014.
[24] Baufeld, O. Van der Biest, and R. Gault, "Additive manufacturing of Ti–6Al–4V components by shaped metal deposition: Microstructure and mechanical properties," Materials & Design, vol. 31. pp. S106–S111, 2010.
[25] B. Lu et al., "Effect of La2O3 addition on mechanical properties and wear behaviour of NiTi alloy fabricated by direct metal deposition," Optics & Laser Technology, vol. 129. p. 106290, 2020.
[26] H. Tan, T. Hu, F. Zhang, Y. Qiu, and A. T. Clare, "Direct metal deposition of satellited ti-15Mo: Microstructure and mechanical properties," Adv. Eng. Mater., vol. 21, no. 8, p. 1900152, Aug. 2019,
[27] P. Åkerfeldt, M.-L. Antti, and R. Pederson, "Influence of microstructure on mechanical properties of laser metal wire-deposited Ti-6Al-4V," Mater. Sci. Eng. A Struct. Mater., vol. 674, pp. 428–437, Sep. 2016,
[28] S. Liu and Y. C. Shin, "The influences of melting degree of TiC reinforcements on microstructure and mechanical properties of laser direct deposited Ti6Al4V-TiC composites," Mater. Des., vol. 136, pp. 185–195, Dec. 2017,
[29] Y. Liu and Y. Zhang, "Microstructure and mechanical properties of TA15-Ti2AlNb bimetallic structures by laser additive manufacturing," Mater. Sci. Eng. A Struct. Mater., vol. 795, no. 140019, p. 140019, Sep. 2020
[30] F. Zhang, M. Yang, A. T. Clare, X. Lin, H. Tan, and Y. Chen, "Microstructure and mechanical properties of Ti-2Al alloyed with Mo formed in laser additive manufacture," Journal of Alloys and Compounds, vol. 727. pp. 821–831, 2017.
[31] S. S. Al-Bermani, M. L. Blackmore, W. Zhang, and I. Todd, "The origin of microstructural diversity, texture, and mechanical properties in electron beam melted ti-6Al-4V," Metall. Mater. Trans. A, vol. 41, no. 13, pp. 3422–3434, Dec. 2010,
[32] K. Syed, M. Awd, F. Walther, and X. Zhang, "Microstructure and mechanical properties of as-built and heat-treated electron beam melted Ti–6Al–4V," Mater. Sci. Technol., vol. 35, no. 6, pp. 653–660, Apr. 2019.
[33] B. Lu et al., "Influence of microstructure on phase transformation behavior and mechanical

properties of plasma arc deposited shape memory alloy," Materials Science and Engineering: A, vol. 736. pp. 130–136, 2018.

[34] H. Suo, Z. Chen, J. Liu, S. Gong, and J. Xiao, "Microstructure and mechanical properties of Ti-6Al-4V by electron beam rapid manufacturing," Rare Met. Mater. Eng., vol. 43, no. 4, pp. 780–785, Apr. 2014.

[35] J. J. Lin et al., "Microstructural evolution and mechanical properties of Ti-6Al-4V wall deposited by pulsed plasma arc additive manufacturing," Mater. Des., vol. 102, pp. 30–40, Jul. 2016.